Interaction between the Z-Type DNA Duplex and 1,3-Propanediamine: Crystal Structure of d(CACGTG)$_2$ at 1.2 Å Resolution[†,‡]

Narendra Narayana,*[,§] N. Shamala,*[,||] Krishna N. Ganesh,[⊥] and M. A. Viswamitra[||,@]

Department of Biochemistry, Case Western Reserve University, Cleveland, Ohio 44106, Department of Physics, Indian Institute of Science, Bangalore 560 012, India, and Division of Organic Chemistry (Synthesis), National Chemical Laboratory, Pune 411 008, India

Received August 7, 2005; Revised Manuscript Received November 12, 2005

ABSTRACT: The crystal structure of a hexamer duplex d(CACGTG)$_2$ has been determined and refined to an *R*-factor of 18.3% using X-ray data up to 1.2 Å resolution. The sequence crystallizes as a left-handed Z-form double helix with Watson−Crick base pairing. There is one hexamer duplex, a spermine molecule, 71 water molecules, and an unexpected diamine (Z-5, 1,3-propanediamine, $C_3H_{10}N_2$) in the asymmetric unit. This is the high-resolution non-disordered structure of a Z-DNA hexamer containing two AT base pairs in the interior of a duplex with no modifications such as bromination or methylation on cytosine bases. This structure does not possess multivalent cations such as cobalt hexaammine that are known to stabilize Z-DNA. The overall duplex structure and its crystal interactions are similar to those of the pure-spermine form of the d(CGCGCG)$_2$ structure. The spine of hydration in the minor groove is intact except in the vicinity of the T5A8 base pair. The binding of the Z-5 molecule in the minor grove of the d(CACGTG)$_2$ duplex appears to have a profound effect in conferring stability to a Z-DNA conformation via electrostatic complementarity and hydrogen bonding interactions. The successive base stacking geometry in d(CACGTG)$_2$ is similar to the corresponding steps in d(CG)$_3$. These results suggest that specific polyamines such as Z-5 could serve as powerful inducers of Z-type conformation in unmodified DNA sequences with AT base pairs. This structure provides a molecular basis for stabilizing AT base pairs incorporated into an alternating d(CG) sequence.

Z-DNA is a left-handed double-helical molecule with Watson−Crick base pairs and an antiparallel organization of the sugar−phosphate chains. The first Z-DNA structure of the hexanucleoside pentaphosphate (dC-dG)$_3$ was determined by X-ray diffraction studies at atomic resolution (*1*). This structure was found to be strikingly distinct from the right-handed double-helical B-form of DNA, which is the predominant form in biological systems. The interconversion of right-handed B-DNA to left-handed Z-DNA was first detected by changes in the circular dichroism of poly(dG-dC) in a high-salt solution (*2*). The right-handed B-DNA to left-handed non-B-DNA transition occurs in sequences containing d(CA/GT)$_n$, found in eukaryotic genomes (*3*−*6*). Z-DNA has been detected by a number of physical (*1*, *2*), chemical (*7*, *8*), and biological methods (*9*). Raman spectroscopic studies have shown that the inversion of poly-(dG-dC) in a high-salt solution bears the same conformation as Z-DNA in the crystal (*10*). The finding that Z-DNA existed under conditions of negative superhelical stress introduced the left-handed conformation within the realm of biological systems (*8*, *11*). Extensive research spanning more than two decades has aided our understanding of the biology, chemistry, and structure of Z-DNA, including the discovery of Z-DNA binding proteins (*12*).

Z-DNA is a higher-energy conformer compared to B-DNA. The energy of negative supercoiling in closed circular plasmids is thought to stabilize a small segment of Z-DNA (*13*). The chemical modifications on the cytosine base, such as bromination or methylation on the C5 position, are known to favor the B-to-Z transition (*14*−*16*). Cations such as cobalt hexaammine (*17*) and spermine (*18*) stabilize the Z conformation. Further, the minor groove spine of hydration is implicated in the stability of Z-DNA. In most cases, the B-to-Z conversion has been observed in polynucleotides with alternating dC and dG bases. In the presence of AT base pairs, this transition is difficult even at very high salt concentrations (*19*−*21*). However, AT base pairs, for example, in sequences such as d(CA)$_n$ are widely found in eukaryotic genomes (*22*, *23*), in contrast to alternating d(CG)$_n$ sequences which are uncommon in biological systems. The Z conformation has been observed in polynucleotides containing AT base pairs through the use of antibodies specific for Z-DNA (*24*). Sections of DNA in the eukaryotic genome with the sequence (dC-dA/dG-dT) (*22*) have been shown to form Z-DNA using both immunological and gel

[†] N.N. thanks the Ohio Cancer Research Associates and American Cancer Society for support. We thank DBT and CSIR (India) for support.

[‡] Atomic coordinates and structure factors have been deposited in the Protein Data Bank (entry 2F8W) and the Nucleic Acid Data Bank (entry ZD0016).

* To whom correspondence should be addressed. Phone/Fax: (216) 368-8740. E-mail: nxn17@case.edu or shamala@physics.iisc.ernet.in.

[§] Case Western Reserve University.

[||] Indian Institute of Science.

[⊥] National Chemical Laboratory.

[@] Deceased. We dedicate this paper to the memory of the late Professor M. A. Viswamitra.

10.1021/bi051569l CCC: $33.50
Published on Web 01/07/2006

electrophoretic methods (*3*, *4*). The d(CACGTG) E-box sequence is the binding site for many transcription factors, including Myc, Max, and others (*25*). Structural studies of d(CA/TG)$_n$ have thus become increasingly interesting in eukaryotic transcription. Z-DNA is generally associated with alternating C-G sequences (*1*, *26*, *27*). Several Z-DNA X-ray structures of oligonucleotides containing AT base pairs have been determined recently. However, except for the palindromic sequences d(CACGTG)$_2$ (*28*) and d(TGCGCA)$_2$ (*29*, *30*) and asymmetric sequences d(CACGCG)·d(CGCGTG), d(CGCACG)·d(CGTGCG) (*31*, *32*), and d(CGCGCA)·d(TGCGCG) (*33*), all other Z-type crystals with AT base pairs have either 5-methylated or 5-brominated cytosine residues which are known to strongly favor the Z-DNA conformation (*15*) or found disordered with cobalt hexammine which stabilizes the Z-DNA conformation (*17*).

In this paper, we describe the crystal structure of a hexanucleoside pentaphosphate, the d(CACGTG)$_2$ duplex complexed with a ubiquitous biological cation, spermine, at 1.2 Å resolution. This sequence possesses d(CA) and d(TG) dinucleotide fragments that are found to recur in eukaryotic systems (*22*, *23*). We compare our structure with the structure determined at 2.5 Å resolution for the same sequence by Coll et al. (*28*) and the canonical Z-DNA structures of d(CG)$_3$: magnesium (*34*), pure-spermine (*18*), and mixed magnesium/spermine (*1*) forms. We discuss the stability of AT base pairs in the Z form in the light of our high-resolution structure with the well-determined water network, intermolecular interactions, and an unexpected diamine found in the crystal.

MATERIALS AND METHODS

Oligonucleotide Synthesis and Purification. The d(CACGTG) oligomer was synthesized in milligram quantity by solution-phase phosphotriester chemistry using a block coupling approach (*35*). The appropriately protected phosphotriester blocks corresponding to dimers TpG, CpG, and CpA were sequentially assembled in a 3′−5′ order, employing synthetic cycles, each consisting of a coupling step using MSNT (mesitylene sulfonyl nitrotriazole) and *N*-methylimidazole, followed by 5′-detritylation with phenyldihydrogen phosphate. The protected hexamer was converted into the free d(CACGTG) oligomer by successive treatment with oximate reagent and ammonia, followed by gel filtration over Sephadex G-15. The void volume eluant was lyophilized and the residue purified by FPLC (Pharmacia) employing a preparative Mono Q anion-exchange column (Pharmacia) and using a solvent gradient of 0.1 M aqueous NaOH (pH 12.0) to 0.1 M aqueous NaOH containing 0.8 M NaCl at a flow rate of 1.5 mL/min. The pure oligomer was recovered by neutralization of the corresponding peak fraction with dilute HCl (1:1) followed by desalting over Sephadex G-15.

Crystallization. Lyophilized flakes of d(CACGTG) were dissolved in doubly distilled water. A single crystal suitable for X-ray diffraction was grown by vapor diffusion at 18 °C using the sitting-drop method. The crystallization mixture contained 1.0 mM d(CACGTG) (single-strand concentration), 7.5 mM sodium cacodylate buffer (pH 6.5), 2.5 mM $SrCl_2$, and 2.5 mM spermine. This mixture was equilibrated against 50% (v/v) 2-propanol. Rectangular, blocklike crystals were grown in ~2 weeks. One crystal 0.76 mm × 0.32 mm × 0.20 mm in size was mounted in a 0.5 mm sealed Lindemann capillary with a droplet of mother liquor and used for X-ray intensity data collection (see the Supporting Information).

Diffraction Data Collection and Processing. The crystal belongs to the $P2_12_12_1$ space group with the following dimensions: $a = 18.42$ Å, $b = 30.74$ Å, and $c = 43.18$ Å. There are two strands (one duplex) per asymmetric unit. These cell dimensions are similar to those of the pure-spermine form of d(CG)$_3$, suggesting an isomorphous structure (*18*). Three-dimensional X-ray intensity data up to 1.2 Å resolution were collected at 18 °C on an Enraf-Nonius CAD-4 diffractometer using the $\omega/2\theta$ scan at 5 kW power ($\lambda_{CuK\alpha} = 1.5418$ Å). Raw intensity data were reduced using the standard package associated with the CAD-4 diffractometer. The data were corrected for Lorentz and polarization effects. The total number of observable reflections with F values greater than 2σ between 50 and 1.2 Å was 5687.

Structure Solution and Refinement. The unit cell dimensions are similar to those of the pure-spermine form of d(CG)$_3$ (*18*). Accordingly, the coordinates of that hexamer (PDB[1] entry 1D48) with appropriate changes in the sequence were used as a starting model in the structure refinement. Rigid-body refinement was performed using X-PLOR (*36*). The *R*-factor converged to 24% for 8−3 Å resolution using 2σ data with an overall *B*-factor of 15.0 Å^2. At this stage, the $2F_o - F_c$ map was computed and displayed on the Silicon Graphics system. The atoms were moved to match the electron density using TOM-FRODO (*37*). In general, the phosphates, bases, and sugar moieties were seen at 3σ, 2.5σ, and 2.0σ, respectively. Simulated annealed molecular dynamics refinement was performed with a starting temperature of 3000 K, and the "slow-cool" protocol was run to 300 K with a decrement in T (ΔT) of 50 K per time step of 0.5 fs (*38*). Several rounds of alternate refinement and electron density fitting were performed with the gradual increment in resolution, until the structure converged to an *R*-factor of 24.6% for data between 8 and 1.2 Å resolution. Omit maps were calculated with each base pair removed at a time, and the base pairs which were removed in the calculation were fitted into the density seen for it. A difference Fourier map at this stage clearly showed the location of a spermine molecule bound to the DNA duplex. Both $F_o - F_c$ and $2F_o - F_c$ maps were used to locate solvent molecules. Only peaks that were well-shaped, had a minimum value of 3σ in the $F_o - F_c$ map and at least 1.5σ in the $2F_o - F_c$ map, and were within 2.5−3.3 Å of possible hydrogen-bonding partners were accepted as water oxygens. In 10 rounds of alternate refinement and location of water molecules, a total of 71 water molecules were found. It was not possible to identify strontium or sodium ions that were used in the crystallization mixture.

The final difference Fourier map computed using the phases obtained from the DNA duplex, a spermine molecule, and 71 water molecules clearly showed well-defined and continuous electron density at $\sim 3.5\sigma$ for an unexpected molecule with a chemical formula of $C_3N_2H_{10}$ (Figure 1)

[1] Abbreviations: HA2, d(CACGCG)·d(CGCGTG); HA4, d(CGCACG)·d(CGTGCG); MPD, 2-methyl-2,4-pentanediol; PA24, *N*-(2-aminoethyl)-1,4-diaminobutane; PA(222), *N*(1)-[2-(2-aminoethylamino)ethyl]ethane-1,2-diamine; PDB, Protein Data Bank; rmsd, root-mean-square deviation; Z-AT, d(CACGTG)$_2$; Z-SP, d(CGCGCG)$_2$ pure-spermine form; Z-5, 1,3-propanediamine ($C_3H_{10}N_2$).

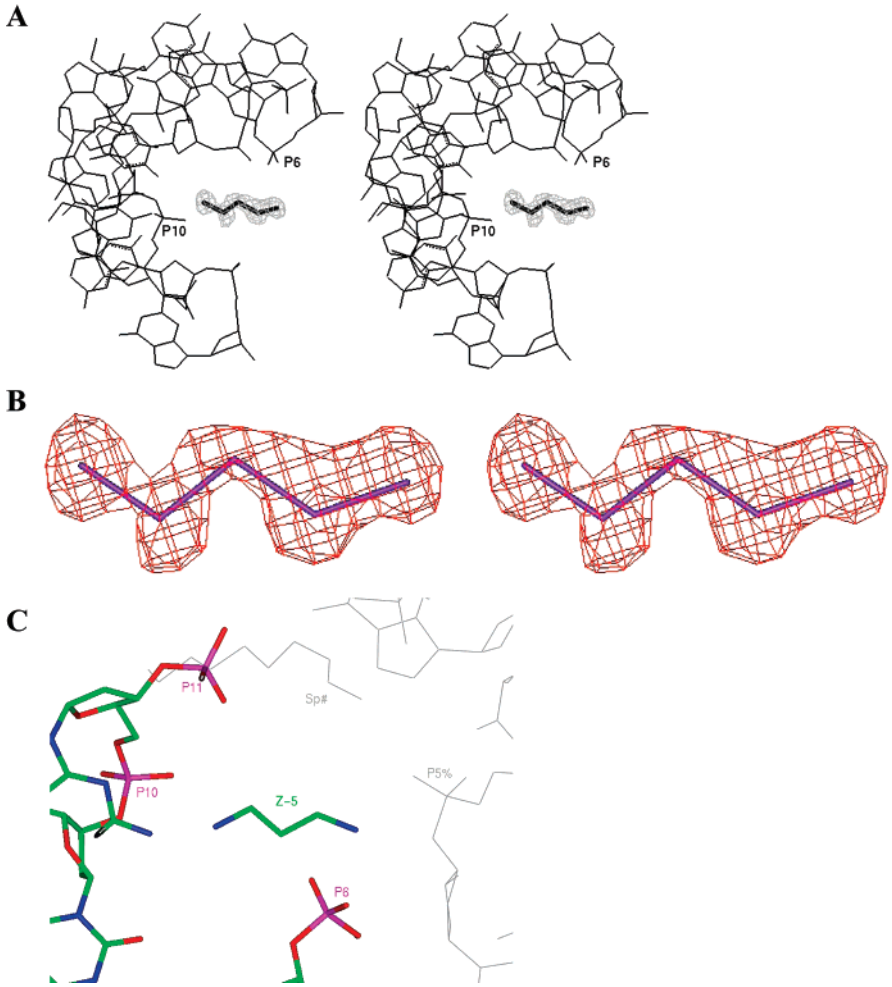

FIGURE 1: (A) Stereoview of the superimposed Z-5 molecule in the difference Fourier map. Electron density map computed using the $F_o - F_c$ coefficients and α_c obtained from a model containing all non-hydrogen atoms from the duplex, spermine, and 71 water molecules. Well-defined, continuous, and strong density at 4σ shows the presence of an unexpected molecule (Z-5, $C_3H_{10}N_2$, 1,3-propanediamine) in the crystal. The Z-5 indicated by thick lines is bound in the deep minor groove involved in hydrogen bonding interactions with phosphate groups of residues G6 and G10. The duplex is depicted with thin lines. (B) Close-up view of the Z-5 molecule superimposed on the difference electron density map contoured at 4σ. (C) Original Z-5 molecule and duplex shown as split-bond sticks (C atoms are colored green, N atoms blue, O atoms red, and P atoms purple). Z-5 is surrounded by phosphate groups from the parent duplex as well as from a symmetry-related duplex (P5%) as seen in the figure. Portions of the two symmetry-related duplexes are shown as gray lines. Symmetry-related spermine (Sp#) is in the vicinity of Z-5. Both polycations spermine and Z-5 fill in the pocket that is surrounded by negatively charged phosphate groups contributing to neutralization of negative charges. Figures 1−4 were generated using InsightII.

that matches the chemical formula of 1,3-propanediamine. We have abbreviated this molecule as Z-5 in our discussions. The atom types in this molecule were assigned on the bases of its interactions with the DNA and water molecules, and by consideration of the permissible bond orders, lengths, and angles between the atoms. The Z-5 molecule in large part is involved in hydrogen bonding interactions with the original DNA duplex and has few interactions with the neighboring duplexes (Figure 2).

Further refinement using X-PLOR included one duplex (240 non-hydrogen atoms), a spermine molecule (14 non-hydrogen atoms), 71 water oxygens, and five non-hydrogen atoms of the Z-5 molecule. Structure refinement was concluded with 20 cycles of positional, 15 cycles of overall *B*-factor, and 20 cycles of individual isotropic *B*-factor refinement. The crystallographic *R*-factor converged at 18.3% with an R_{free} of 21.5% for 2σ data up to 1.2 Å resolution with good geometrical parameters. A summary of crystal data and structure refinement is provided in Table 1. The relative average isotropic thermal factors (*B* values) are overall as follows: all non-H atoms, 14.8 Å^2; DNA atoms, 6.9 Å^2; phosphate groups, P, O1P, O2P, O3′, and O5′, 9.9 Å^2; deoxyribose sugars, 6.8 Å^2; bases, 5.6 Å^2; water molecules, 41.7 Å^2; spermine, 12.0 Å^2; and Z-5 molecule, 23.6 Å^2. The rmsd's from standard geometry for bond lengths, bond angles, dihedral angles, and improper angles are 0.013 Å, 3.18°, 32.14°, and 1.32°, respectively. The electron density maps did not reveal features of coordination geometry for the divalent strontium ions.

RESULTS

Overall DNA Structure. The crystallographic asymmetric unit consists of two chemically identical self-complementary hexanucleoside pentaphosphate strands forming an antiparallel duplex with six Watson−Crick base pairs. The helix is of the left-handed Z-DNA type with structurally independent strands. This is the first unmodified Z-DNA hexamer structure (Figure 3) containing two AT base pairs in the interior of the duplex determined at high resolution (Bragg spacing of 1.2 Å). DNA residues are numbered in the 5′−3′

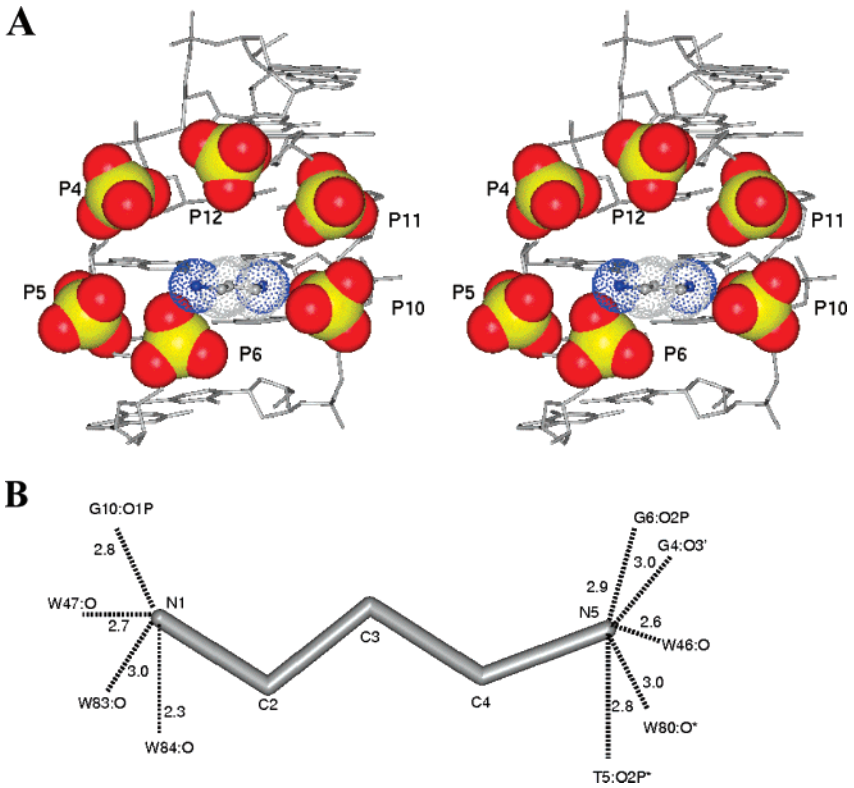

FIGURE 2: Environment of the bound Z-5 molecule. (A) Stereoview of the bound Z-5 molecule in the minor groove of the d(CACGTG)$_2$ duplex (gray sticks). Six negatively charged phosphate groups (CPK representation) provide favorable electrostatic attraction to the positively charged polyamine Z-5 (dotted CPK spheres). The planar Z-5 molecule forms an interstrand bridge between residues G6 and G10. The two terminal amino nitrogen atoms (blue spheres) are hydrogen-bonded to cross-strand phosphate oxygen atoms. The methylene groups (gray spheres) are not involved in hydrophobic interactions with the DNA atoms and appear to serve as an optimal spacer between the terminal amino groups that interact with the phosphate oxygen atoms. (B) Schematic diagram showing the interactions involving Z-5. Z-5 is shown as gray sticks. The hydrogen bonds (angstroms) are indicated by hatched lines. The asterisk denotes the symmetry-related atom. In addition to intrahelical groove interactions, Z-5 is involved in interduplex interactions in the crystal lattice; N5 makes an ionic interaction with the symmetry-related phosphate oxygen of T5. The water molecules are designated by the letter W.

Table 1: Crystal Data and Summary of Refinement Parameters

oligonucleotide	d(CpApCpGpTpG)
molecular formula per strand	$C_{58}H_{76}N_{23}O_{34}P_5$
molecular weight	1794.4
radiation	Cu Kα ($\lambda = 1.5418$ Å)
crystal size	0.76 mm × 0.32 mm × 0.20 mm
space group	$P2_12_12_1$
cell dimensions	$a = 18.42$ Å, $b = 30.74$ Å, and $c = 43.18$ Å
unit cell volume	24449.8 Å^3
no. of DNA molecules/ asymmetric unit	two strands of d(CACGTG)
solvent content	28%
data collection method	$\omega/2\theta$ scan on a CAD-4 diffractometer
temperature	18 °C
resolution	6.0−1.2 Å
no. of unique reflections ($F > 2\sigma_F$)	5687
R_{sym}	4.2%
R-factor[a]	18.3%
R_{free}[a]	21.5%
total no. of non-H atoms	330
DNA	240
spermine	14
1,3-propanediamine	5
water oxygens	71

[a] Agreement index $R = 100\Sigma|F_o - F_c|/\Sigma F_o$.

direction from C1 to G6 for strand A and from C7 to G12 for strand B. Residue 13 is spermine; water molecules are labeled W14−W84, and an unexpected diamine molecule (Z-5, 1,3-propanediamine) is residue 85. For convenience in comparing it with the relevant Z-DNA structure, we abbreviate the d(CACGTG) structure described in this paper as Z-AT and that of the pure-spermine form of d(CG)$_3$ as Z-SP. The Z-AT structure most closely resembles the structure of Z-SP (see the Supporting Information) (*18*). The rmsd of DNA atomic positions (non-H atoms) between Z-AT and Z-SP is 0.57 Å. The rmsd of atomic positions of the two chemically equivalent DNA strands in the Z-AT structure is 0.79 Å, in comparison with a value of 0.98 Å reported for the Z-SP structure. The Z-AT crystal is isomorphous to the Z-SP crystal, whereas the crystals of d(CACGTG) determined at 2.5 Å resolution (*28*) are isomorphous to d(CGCGCG)$_2$ magnesium (*34*) and mixed magnesium/spermine (*1*) forms. Both Z-AT and Z-SP duplexes are shorter than the magnesium form of the d(CGCGCG) duplex (including other Z-DNA hexamers crystallized so far). The average helical rise in Z-AT is 3.61 Å in comparison with values of 3.67 Å in the Z-SP form, 3.80 Å in the magnesium form, and 3.89 Å in the mixed spermine/magnesium form. Consequently, a complete turn of a Z-DNA helix (12 base pairs) of Z-AT would be 3.08 Å shorter than a full turn of the mixed magnesium/spermine form. The helical twists in Z-AT and Z-SP are the same with 11.92 and 11.96 residues per turn, respectively. These two structures are slightly overwound in comparison with the magnesium and magnesium/spermine forms exhibiting 12.08 and 12.06 residues per turn, respectively. The duplex displays a major groove that resembles a convex

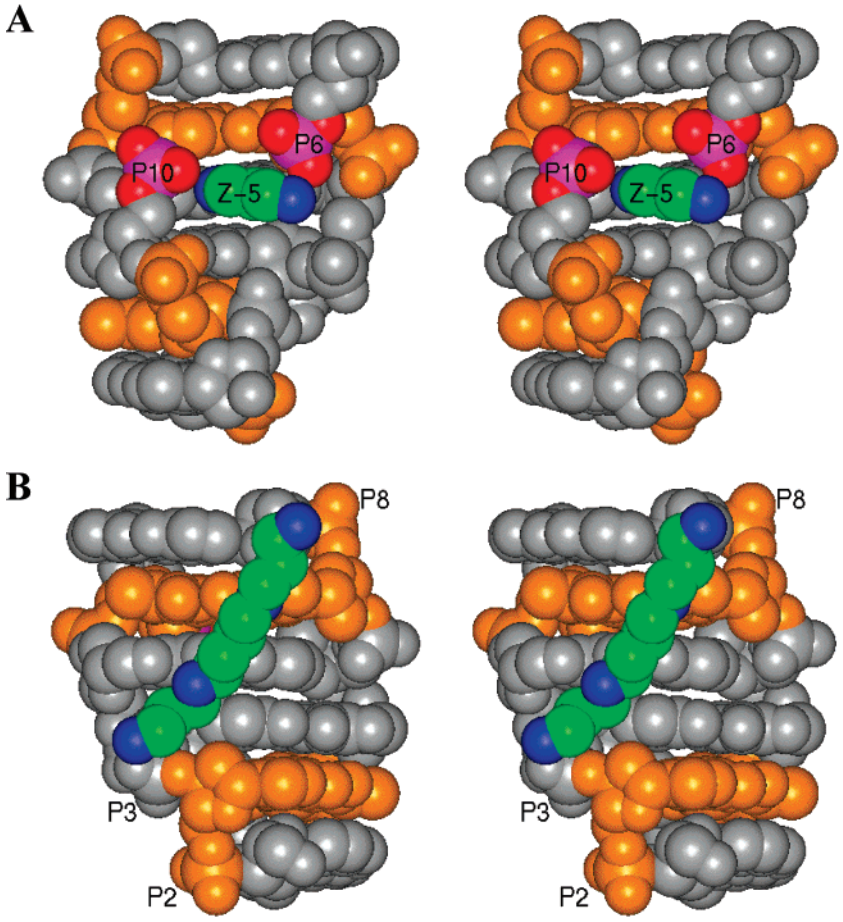

FIGURE 3: 3. Overall view of the d(CACGTG) duplex. (A) Stereoview of the CPK representation of the molecular structure of $d(CACGTG)_2$ and the minor groove-bound diamine Z-5 molecule. The AT base pairs and the associated sugar−phosphate backbones are colored gold. The carbon and nitrogen atoms in Z-5 are colored green and blue, respectively. The phosphate moieties in contact with the amino nitrogen atoms of Z-5 are colored red (phosphate oxygen atoms) and purple (P6 and P10 phosphorus atoms). The remaining atoms in the DNA molecule are colored gray. (B) Stereoview of the CPK representation of the molecular structure of $d(CACGTG)_2$ with bound spermine on the major groove side. Residues A2, T5, A8, and T11 are colored gold and the remaining DNA residues gray. The carbon and nitrogen atoms of the spermine that span between the phosphate groups of residues C3 and A8 are colored green and blue, respectively. The phosphate atoms of residues 2, 3, and 8 are labeled.

surface and a deep and narrow minor groove as seen in canonical Z-DNA structures. The availability of high-resolution data has led us to determine the precise positions of the bound polyamines, solvent molecules, and detailed DNA geometry. The overall environment of the duplex in the crystal resembles that seen in the Z-SP structure and is different from that of the magnesium and mixed magnesium/spermine forms. As in other Z-DNA structures, the polyamine cations and the polar water molecules provide electrostatic complementarity for the overall anionic nature of the Z-duplex.

Base Pair and Step Geometry. Sequence-specific structural features are manifested by the organization of the bases in the interior of the double helix. The glycosidic torsion angle (χ), O4′−C1′−N1−C2 for pyrimidine bases and O4′−C1′−N9−C4 for purines in the structure presented here, follows the standard pattern of anti and syn conformation at pyrimidine and purine residues, respectively. In general, the other base pair and base step-related parameters such as propeller twist, buckle, tilt, roll, and slide show no significant variation compared to those of Z-SP, indicating excellent integration of A-T base pairs within the canonical Z-DNA containing C-G base pairs (see the Supporting Information). It is interesting to note that the propeller twist of the A2-T11 base pair is quite different (−5.76°) compared to that of Z-SP (−0.03°). The buckles at base pairs A2-T11 (9.70°) and T5-A8 (−9.41°) have values that are significantly different from the corresponding values in Z-SP (4.55° and −2.45°, respectively). The six Watson−Crick base pairs exhibit normal hydrogen bonding distances ranging between 2.7 and 2.9 Å.

Sugar−Phosphate Backbone. In general, the conformation angles follow the trend found in the Z-SP structure. The major deviation from the Z-SP structure occurs at bases G4, A8, and C9. The angle ζ (C3′−O3′−P−O5′) at G4 differs considerably from the corresponding angle in Z-SP by 13°. Torsion angles ϵ (C4′−C3′−O3′−P) and ζ at A8 exhibit quite different conformations compared to the equivalent angles in Z-SP with values differing by 46° and 252°, respectively. Torsion angle β (P−O5′−C5′−C4′) at base C9 assumes a conformation significantly different from that of the Z-SP structure with a deviation of 68°. Usually, the pyrimidine and purine bases are associated with C2′-endo and C3′-endo sugar pucker, respectively, in the Z-type DNA. In the structure presented here, except for the terminal G6, C7, and G12 residues, other residues assume the expected geometries. The sugars at G6, C7, and G12 adopt C2′-endo, C1′-exo, and C2′-endo conformations, respectively. The deoxyribose conformation of these residues in Z-SP is C2′-

endo. The sugar−phosphate backbones in Z-DNA structures typically exhibit two distinct sets of torsional angles, one for pyrimidine residues and the other for purine residues. Thus, regular alternation of torsions is seen in Z-DNA sequences with alternating pyrimidine and purine residues. The ZI type corresponds to such an alternating pattern of backbone torsion angles in Z-DNA. In some cases, specific torsion angles such as α, β, ϵ, and ζ in a contiguous pyrimidine-purine stretch adopt similar values resulting in a ZII-type backbone. In the structure presented here, purine residue A8 displays a conspicuous difference in ϵ and ζ compared to the corresponding values in Z-SP. Torsion angle ζ values of C7 and A8 are similar in this structure. Thus, the structure presented here displays a mixed ZI (strand A)/ZII (strand B) conformation for the sugar−phosphate backbone. Torsion angle α at residue C9 differs by 25° compared to the corresponding value in Z-SP. The backbone geometry of both strands for most part is as seen previously in other Z-DNA hexamers. The phosphate moiety of residue C9 assumes the ZII conformation. Apart from these differences in the backbone conformation of strands A and B, the backbone torsion angles closely conform to 2-fold symmetry relating two palindromic strands (see the Supporting Information).

Hydration. The Z-DNA duplex is surrounded by water molecules in addition to the bound polycations: spermine and the Z-5 molecule (Figure 4). The water molecules are densely populated on the minor groove of the duplex (Figure 4B), whereas the water molecules are sparsely distributed on the major groove face (Figure 4C). A total of 71 ordered water molecules were located in the difference Fourier maps. Of these, 44 water molecules are positioned along the minor groove and 27 water molecules span the major groove. The minor groove hydration exhibits several layers of ordered water molecules that are involved in hydrogen bonding with nucleotide bases, sugars, phosphates, other water molecules, and the polyamine Z-5. All water molecules are involved in multiple contacts with most of them displaying the stable tetrahedral geometry (see the Supporting Information). The average *B*-factor for water molecules is 41.7 Å^2. The present Z-DNA structure containing two AT base pairs embedded within the 6 bp duplex displays hydration patterns similar to those described in high-resolution Z-DNA structures with alternating d(CG) base pairs. Several water bridges consisting of one or more water molecules link the polar functional groups of the DNA duplex.

In addition to spermine, 27 water molecules are observed on the flat surface of the major groove (Figure 4C). Both the base and the sugar−phosphate backbone atoms share almost equally the number of observed hydrogen bonding interactions with the water molecules. Water structure motifs are seen on both minor and major grooves as described previously by Egli and colleagues (*39*). It is interesting to note that a roughly planar pentagonal ring of hydrogen bonds is formed in this region where the vertexes of the pentagon are C7 O2, A6 N2, W39, W42, and W66 (Figure 4A). To the best of our knowledge, this is the first reported observation of a pentagonal ring in Z-DNA. This pentagonal pattern is reminiscent of fused pentagons of water molecules seen in the major groove of A-DNA (*40*). The ordered network of water molecules may further stabilize the Z helix.

Spermine−DNA Interaction. Spermine is a natural polyamine with 14 functional groups (amino, imino, and methylene) linked linearly via single covalent bonds. The highly flexible spermine molecule (*41*) has a net charge of +4 at pH 7 and serves to neutralize the polyanionic character of the sugar−phosphate backbones in addition to hydrogen bonding with base atoms and water molecules. In the structure presented here, spermine assumes an extended zigzag conformation, diagonally spanning the major groove surface (Figures 3B and 4C). Each of the amino and imino groups in the spermine molecule interacts with a phosphate moiety either directly or indirectly through a bridging water molecule. Both the amino and imino groups hydrogen bond with several symmetry-related water molecules. Of a total of 14 polar interactions within 3.5 Å, only four of them (13 N1···C3 O2P, 13 N5···W19, 13 N10···A8 N7, and 13 N10···W36 bonds) are with the parent molecule and the remaining are with the symmetry-related atoms. This feature highlights the role of the spermine molecule in the intermolecular interactions. The overall conformation and the binding mode of spermine are similar to those found in the crystal structure of the pure-spermine form of d(CGCGCGC)$_2$ except in the N10−N14 stretch where significant variations occur. On the basis of its direct and indirect interactions with several phosphate groups, it is presumed that spermine is a major contributor to packing of DNA duplexes via electrostatic complementarity.

Z-5−DNA Interaction. The minor groove strip between phosphate groups of residues 6 and 10 is filled by a small zigzag-shaped polycation with a molecular formula of $C_3H_{10}N_2$ and a molecular weight of 74.13 (Figure 2). It has an amino group at the ends and three methylene groups between the ends. The presence of this molecule in the electron density map was surprising and unexpected (Figure 1). The structural formula of this molecule (Figure 2B) reveals a polycation with the right length and chemical properties to be accommodated in the minor groove. The atomic types were assigned on the bases of its hydrogen bonding interactions. We assume that it carries a net positive charge analogous to that of the spermine molecule at neutral pH because of its direct binding to two closely spaced phosphate anions and its presence in a region with high negative potential because of the six surrounding phosphate anions (Figure 2A). We do not know the origin of this substance or how it was introduced into our crystallization mixture. We were unable to reproduce the crystals later using freshly prepared oligonucleotide, buffer, salt, spermine, and MPD solutions. It is readily seen from comparison of the structural formula of Z-5 (Figure 2B) with that of spermine that this fragment mimics the truncated version (N1−C2−C3−C4−N5) of the whole length spermine, where N1 and N5 denote amino and imino groups, respectively, and C2−C4 denote methylene groups. In Z-5, N5 is an amino group instead of an imino group in the corresponding position in spermine. It is unlikely that the fragment seen is a part of the spermine molecule because the extension of the fragment would result in unfavorable geometry and steric clashes. The binding of the Z-5 molecule in the minor groove (Figures 2A and 3A) may help to stabilize the nonmodified AT base pair (T5-A8) sandwiched between G4-C9 and G6-C7 base pairs and concomitantly enhance the diffraction quality of the crystals. We do not see the binding of the Z-5 molecule near the other nonmodified AT base pair (A2-T11) sandwiched between C1-G12 and C3-G10 base pairs, indicating

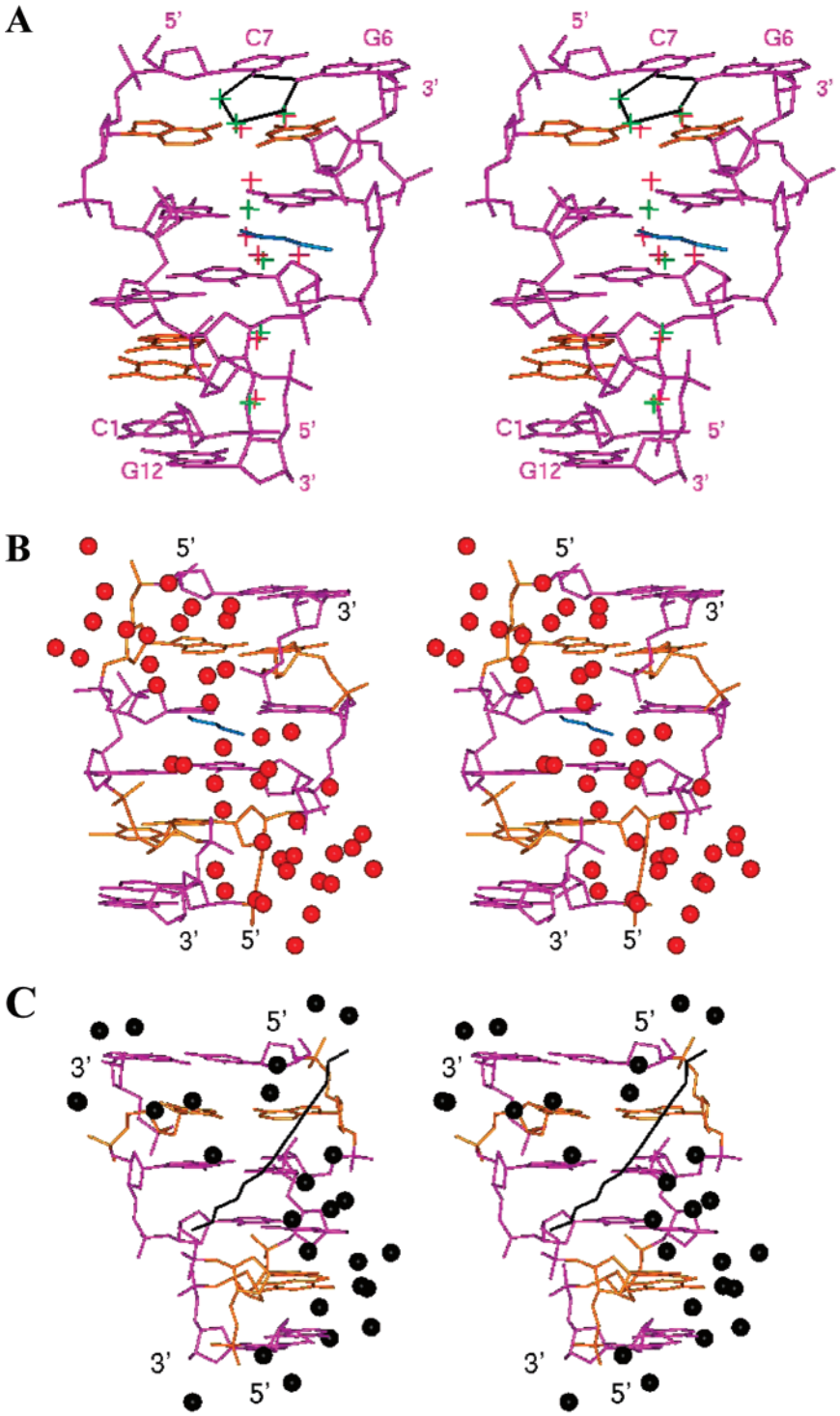

FIGURE 4: 4. Stereoview of the minor and major groove hydration. (A) The AT base pairs are colored gold, while the CG base pairs are colored purple. The spine of hydration seen at the floor of the minor groove is shown for both Z-AT and Z-SP structures. The water molecules in the present structure (Z-AT) are colored green, and those observed in the pure-spermine form of the parent sequence Z-SP are colored red. The Z-5 molecule is displayed as cyan sticks. A pentagonal array of hydrogen bonds (black lines) is seen at one end of the duplex. Such a pattern may contribute to the helix stability (*40*). (B) Minor groove hydration observed in the crystals of the d(CACGTG) duplex. Water oxygen atoms on the minor grove face are colored red. (C) Major groove hydration in this structure with water oxygens displayed as black spheres. The bound spermine molecule spanning the major groove surface is drawn as black lines. It is clear from panels B and C that the minor groove is densely populated with water molecules compared to the major groove surface.

nonspecific binding. This could be due to a different microenvironment compared to that seen at the T5-A8 base pair and thus not favorable for the binding of Z-5. The amino group at position 1 is involved in interactions with 10 O1P, W47, W83, and W84 of the parent duplex, while the amino group at position 5 interacts with 6 O2P and W46 of the parent duplex and with 4 O3′, 5 O2P, and W80 of the symmetry-related duplex (Figure 2B). Therefore, Z-5 plays a role in both intrahelical and interhelical interactions.

Crystal Packing. The unit cell dimensions of the d(CACGTG)$_2$ crystal presented here are isomorphous to those of the pure-spermine crystal form of d(CGCGCG)$_2$ (*18*). The

crystal packing in this structure closely resembles that of Z-SP. Spermine plays a critical role in establishing interduplex stability as well as in intrahelical electrostatic compensation. The T5 O2P from a symmetry-related sugar−phosphate backbone is involved in an ionic interaction with the N5 amino group of the parent Z-5 molecule. Water-mediated and polyamine-mediated (spermine and Z-5) intermolecular interactions dominate in crystal packing. In addition, the base stacking interactions that exist between the hexamer duplexes forming an infinite chain of duplexes are a major driving force in crystal packing.

It is noteworthy that both Z-5 and symmetry-related spermine are located side by side (Figure 1B) to compensate for the dense negative potential present in the minor groove, where a cluster of six phosphate groups is seen. Spermine is primarily involved in stabilizing the intermolecular interactions in the crystal packing. The Z-5 molecule contributes mainly to the intrahelical stability and also assumes a secondary role in intermolecular interactions via ionic interaction with T5 O2P of a symmetry-related duplex. Metal ions (sodium, magnesium, manganese, calcium, ruthenium, cobalt, etc.) and polyamines (spermine and spermidine) have been used traditionally to help stabilize the DNA conformation that is rich in phosphate ions. This work reveals that smaller polyamines such as Z-5, putrescine (*42*), and others may have a role in stabilizing intrahelical geometry, specifically when the destabilizing AT base pairs are incorporated into alternating CG-rich sequences forming Z-DNA.

DISCUSSION

The initial crystal structures of Z-DNA revealed a surprisingly different conformation compared to the B-DNA structure (*1*, *26*, *27*). Z-DNA is a left-handed duplex with dinucleotide as a repeating unit, whereas B-DNA is a right-handed duplex with mononucleotide as a building block. The Z-type conformation was found in DNA sequences with alternating C and G bases (*1*, *43*). Since the discovery of Z-DNA in hexameric DNA sequence d(CGCGCG)$_2$, several crystal structures of Z-DNA hexamers in different crystalline environments (*1*, *18*, *29*−*31*, *33*, *44*), with metal or polyamine bound (*45*−*47*), and with modified bases (*48*) have been determined. Most of these structures have alternating pyrimidine (C) and purine (G) bases, their modifications such as methylation or bromination at position 5 of cytosine bases, and some with modified A and T bases (for example, substitution of an amino group at position 2 of adenine) in a CG-rich sequence. Recently, few Z-DNA crystal structures with unmodified A and T bases incorporated into sequences containing unmodified C and G bases have been determined (*28*−*33*). Solution studies using circular dichroism have shown that AT base pairs are less stable compared to CG base pairs in the Z-DNA form (*21*). DNA sequences with AT base pairs are significantly more "Z-phobic" than CG base pairs. The free energy cost for changing a CG base pair to an AT base pair in the Z conformation is ∼2−3 kcal/mol more than in the B form (*49*). Because bromination or methylation of cytosine bases strongly stabilizes the Z-DNA conformation (*14*−*16*), physicochemical studies were performed by incorporating AT base pairs into such modified CG sequences.

The first crystal structure of Z-DNA containing AT base pairs, d(m^{5}CGTAm^{5}CG), has offered plausible explanations for its influence in destabilizing the Z form of DNA (*50*). Since then, structures of four Z-DNA hexamers containing AT base pairs and unmodified bases have been determined (*28*−*33*). To better understand the molecular basis of the destabilizing effect of AT base pairs in an alternating pyrimidine-purine sequence, we have determined the crystal structure of DNA hexamer d(CACGTG)$_2$ with two AT base pairs sandwiched between CG base pairs. The structure of d(CACGTG)$_2$ described in this paper is at a higher resolution (1.2 Å vs 2.5 Å) compared to the structure described previously by Coll et al. (*28*). The structure described by them has cell dimensions and overall architecture deviating significantly from those of the structure presented here. In addition, their work indicates that in the absence of spermine, the d(CACGTG) sequence crystallized with quite different cell dimensions and exhibited poor diffraction. Thus, the d(CACGTG) sequence displays structural polymorphism. Since the coordinates of the structure determined by Coll et al. (*28*) are not available in the public domain, we are unable to quantitatively compare our structure with their structure.

The d(CACGTG)$_2$ duplex is compressed as in the pure-spermine form of d(CG)$_3$. The width of the minor groove is similar to that found in the pure-spermine form (see the Supporting Information) and is shorter than those found in magnesium and mixed spermine/magnesium forms. The smaller minor groove width in the d(CG)$_3$−spermine complex was attributed to the presence of a spermine molecule in the minor groove, which weakens the electrostatic repulsion between the negatively charged sugar−phosphate backbones, consequently resulting in a decrease in groove width. In the structure presented here, the Z-5 molecule has the same impact on the minor groove width, helical compression, and increase in the depth of the minor groove as the bound spermine in the low-temperature d(CG)$_3$−spermine complex (*51*).

The stability of a ZII conformation is generally attributed to the metal coordination. The phosphate moiety of residue C9 assumes the ZII conformation (see the Supporting Information), with no signs of divalent cations in the vicinity of the phosphate group. This feature may suggest that ZI and ZII are interconvertible without energy penalty. Crystal packing forces may influence the phosphate geometry. In the pure-spermine form of d(CGCGCG)$_2$, the phosphate group of residue C9 is disordered with ZI as the major conformer and ZII as a minor conformer. The 10 negative charges of the phosphate groups of the d(CACGTG)$_2$ duplex are neutralized by spermine (four positive charges), the Z-5 molecule (two positive charges), and four additional positive charges from sodium or magnesium cations from the buffer and salt solutions in the crystallization solution. However, electron density maps were featureless with regard to characteristic coordination geometry for the metallic cations.

Systematic incorporation of AT base pairs into the canonical Z-DNA sequence containing alternating CG base pairs has been carried out by Gautham and co-workers (*30*−*33*). Their studies have shown that replacement of a single CG base pair with a TA base pair in the canonical Z-DNA hexamer results in sequence-dependent structural variations. The crystal structures of non-self-complementary duplexes d(CACGCG)·d(CGCGTG) (*31*) and d(CGCACG)·d(CGTGCG) (*31*) designated as HA2 and HA4 duplexes, respectively, belong to the Z-DNA conformation similar to the structure

presented here. The average value of the rise per base pair is 3.74 Å in HA2 and 3.58 Å in HA4. The shorter HA4 duplex has the average rise per base pair comparable to that seen in the structure presented here (3.61 Å). The base stacking pattern in HA2 closely resembles the stacking pattern observed in the parent Z-DNA structure like the present $d(CACGTG)_2$ structure. The structure of HA4 deviates considerably from the standard Z-DNA conformation and diffracts poorly in comparison to HA2. Wang et al. (*52*) have proposed that at least four consecutive CG base pairs are required for a stable Z-DNA conformation; in support of this proposition, variations in base stacking observed in HA4 were ascribed to the nonexistence of four contiguous GC base-pairs in the sequence (*31*). In the high-resolution structure presented here, the $d(CACGTG)_2$ sequence which does not fulfill the requirement of four contiguous GC base pairs, nevertheless, adopts a stable Z-DNA conformation. Therefore, we propose that the stability of a specific Z-DNA sequence with AT base pairs is context-dependent rather than the result of the sheer presence of a minimum of four consecutive GC base pairs in the sequence. Two groups have independently determined the structure of $d(TGCGCA)_2$ that contains AT base pairs at the ends in the hexamer (*29*, *30*). The duplex is very similar to the original Z-DNA structure and shows that the replacement of CG base pairs at the ends is well-tolerated. Recently, the structures of d(CGCGCA)·d(TGCGCG) in two crystal forms have been determined (*33*). The helical parameters in this structure are those expected for Z-DNA. The presence of an AT base pair at the end of the duplex does not perturb the overall geometry of the duplex. Thus, the recently growing body of information on Z-DNA hexamers containing AT base pairs suggests that AT base pairs can be accommodated in the Z-type conformation in specific sequences with base modifications, polyamines, and salts.

To our surprise, we found a zigzag-shaped electron density in the minor groove (Figure 1). On the basis of its interactions (Figure 2B), we have interpreted this density as a diamine (Z-5, 1,3-propanediamine) with three methylene moieties between the amino groups at the ends of the molecule. Unlike the spermine molecule, the Z-5 molecule has primary interactions with the parent DNA molecule. This molecule fits snugly in a region surrounded by six phosphate groups (Figures 2A and 3A), and the amino groups are involved in direct contact with phosphate oxygens of the parent and the symmetry-related duplexes. Because of these interactions with the phosphate anions, we presume that the ends of the Z-5 molecule possess a net positive charge of +2, and thus, Z-5 resembles a polyamine. This is the first example of a short polyamine that is bound in the minor groove conferring electrostatic complementarity and consequently enhancing the relative stability of the DNA structure.

Previous studies of the pure-spermine form of $d(CGCGCG)_2$ at a low temperature (−110 °C) (*51*) revealed that the spermine molecule was bound in the minor groove of two hexamer duplexes that are stacked in an end-to-end fashion in the crystal lattice. The binding of the spermine molecule in the minor groove intruded into the spine of hydration and weakened the cross-strand electrostatic repulsion within the helix, resulting in the increased relative stability. In the studies presented here, the binding of the Z-5 molecule does not disrupt the minor groove spine of hydration and is located in a region surrounded by six intrahelical phosphate groups, a "hot spot" for the binding of a positively charged molecule (Figure 2A). The crystal structures of $d(CG)_3$ complexed with spermine, *N*-(2-aminoethyl)-1,4-diaminobutane (PA24), spermidine, thermospermine, and *N*(1)-[2-(2-aminoethylamino)-ethyl]ethane-1,2-diamine [PA(222)] reveal different modes of interaction with the DNA fragment (*44*−*47*, *51*). Further, in the study presented here, the binding mode of Z-5 in the minor groove is different from those seen previously in other polyamine−Z-DNA structures. Although 1,3-propanediamine is known to interact with phosphate moieties (*53*), this work describes for the first time the binding of a diamine to a DNA fragment in crystals. The presence of the polyamine degradation product 1,3-propanediamine as an impurity in our crystallization mixture has enabled us to grow crystals of $d(CACGTG)_2$ that diffracted to high resolution. It may be noted that previous work on the same sequence by Coll et al. resulted in poorly diffracting crystals (*28*) that lack the Z-5 molecule. We were able to grow diffraction-quality crystals of $d(CACGTG)_2$ only once. Reproducing these crystals was difficult and sometimes resulted in microcrystals. We are currently attempting to grow crystals of $d(CACGTG)_2$ by explicit use of 1,3-propanediamine.

The previous room-temperature and low-temperature studies of spermine-bound $d(CG)_3$ (*18*, *51*) have indicated that the spermine in the minor groove is disordered in the room-temperature structure and ordered in the low-temperature structure. It was interpreted that a specific chain of ordered water molecules observed in the minor groove in the room-temperature studies represents the amino/imino groups of spermine and the intervening methylene groups are disordered, and hence invisible in the electron density map. It is possible that such a scenario occurs in our room-temperature studies where a fragment of the spermine molecule is disordered. However, it may be noted that the 1,3-propanediamine in this work spans the helical groove laterally, thus impeding the smooth extension of the molecule on both sides.

This work suggests that the use of a specific polyamine may help stabilize the AT and CG base pairs in the Z-type conformation. Although AT base pairs display less readiness in assuming the Z-type conformation, our study indicates that unmodified AT base pairs can be accommodated into the Z conformation with less resistance in combination with a suitable polyamine. At this point, it is not clear whether the Z-5 molecule alone is sufficient to stabilize the Z conformation of the $d(CACGTG)_2$ duplex or the presence of spermine is also required. Future experiments without spermine in the crystallization trials would help clarify this issue. The binding of spermine to A-, B-, and Z- DNA and its influence on the structural properties highlight the importance of polyamines in the structure and function of DNA (*53*−*56*). Recent studies have shown that 1,3-propanediamine and spermidine enhance the B → A transition, while putrescine and cadaverine repress it, indicating that the trimethylene separation between polyamine charges is important in DNA structural conversion (*53*). These observations imply that intermolecular interactions between the polyamine and DNA play an important role in the structural transitions. Further work on crystallization of Z-DNA fragments, including sequences larger than the hexamer, with designed polyamines may advance our knowledge of the role of polyamines in Z-DNA structure−function relationships.

Raman spectroscopy of d(CACGTG) in solution (B form) and crystal (Z form) shows different conformations (*57*). Furthermore, solution studies employing two-dimensional ^{1}H−^{31}P NMR and circular dichroism spectroscopy by Ganesh and Rajendrakumar (*35*) suggest that d(CACGTG)$_2$ adopts an overall B conformation even at high ionic strengths with concomitant microheterogeneity in local conformation. Some of the possible reasons for the destabilizing effect of AT base pairs in a Z-DNA conformation are discussed below. The replacement of a CG base pair with a TA base pair results in the loss of one hydrogen bond due to the absence of an amino group at position 2 in adenine. For the same reason, a water molecule associated with N2 of guanine is missing in the base pair containing adenine; consequently, the water bridge between the adenine base and the nearby phosphate group is absent. This water bridge in the CG base pair is thought to stabilize the syn conformation of a purine base in Z-DNA. The absence of an N2 amino group in adenine base A8 seems to affect the hydration network in the vicinity, where the spine of hydration in the minor groove is interrupted. However, the spine of hydration at the other end of the duplex that has an A2 base is intact. Thus, if indeed the spine of hydration in the minor groove helps stabilize the Z conformation, the AT base pairs in d(CACGTG)$_2$ appear to be less disruptive to the formation of a spine of waters. It may be possible to restore the missing water in the minor groove spine at one end by replacing T with U because previous work has shown that removal of the methyl group on T helps to restore hydration in the minor groove (*58*). The weaker base stacking interaction involving the adenine base is also related to the missing N2 amino group, resulting in reduced stacking overlap between the bases. Possible reasons for the d(CACGTG) sequence resisting to adopt the Z conformation in solution while it assumes the Z form in crystals are the crystallization conditions and the crystal lattice contacts that are different in the solution studies.

The methylation or bromination at the C-5 position of cytosine is known to overcome the destabilizing effect on the Z conformation precipitated by the incorporation of AT base pairs within a CG-rich sequence. The hydrophobic bonding between the methyl or bromine groups at the C-5 position of cytosine is thought to stabilize the Z form (*59*, *60*). It is apparent from this work that the bound Z-5 molecule through its electrostatic contribution and hydrogen bonding interactions compensates for the destabilizing effects of AT base pairs in Z-DNA. This suggests that apart from base stacking interactions, electrostatic interactions play a key role in stabilizing the architecture of Z-DNA. Systematic structural work by Ohishi et al. (*44*−*47*) has shown different binding modes of polyamines in d(CG)$_3$. This study for the first time highlights the pivotal role played by polyamines in stabilizing the Z-DNA conformation in a sequence different from the canonical Z-DNA and containing AT base pairs that are known to destabilize the Z conformation.

Specific polyamines with certain DNA sequences may stabilize noncontiguous regions of Z-DNA; for example, in the self-complementary DNA dodecamer d(CGCGAATTCGCG), CGCG ends may adopt Z-like structure and the AATT region may adopt either B or an intermediate structure. Previous NMR studies of this sequence with brominated cytosines implied junctions between B- and Z-DNA (*61*). In addition, the use of specific polyamines may help in crystallizing longer than hexamer DNA sequences with ordered structure. In the future, it would be interesting to crystallize unmodified Z-DNA sequences with contiguous AT base pairs and alternating AT and GC base pairs in the presence of Z-5 (or its variants) to study its role in crystallization and stabilizing the Z conformation.

In summary, the presence of AT base pairs in alternating d(CG) sequences has been shown to exhibit sequence-dependent microheterogeneity in Z-DNA (*31*). Gautham and co-workers have been able to determine Z-DNA structures containing AT base pairs in different crystal packing environments, salt conditions, and positions in the hexamer (*30*−*33*). Their structures display sequence-dependent plasticity, and the work of Coll et al. (*28*) shows structural polymorphism. Our work presented here demonstrates the potential of AT base pairs to integrate into the Z-DNA conformation along with CG base pairs without significant distortion from the canonical geometry. Thus, these studies taken together suggest that AT base pairs are malleable and impart sequence-dependent and context-dependent variability or rigidity to Z-DNA.

ACKNOWLEDGMENT

We thank P. K. Srivastava for help in preparing solutions for crystallization experiments. N.N. thanks N. Divya for technical help in manuscript preparation.

SUPPORTING INFORMATION AVAILABLE

Figures showing stereoviews of the least-squares fit of d(CACGTG)$_2$ and d(CGCGCG)$_2$ (pure-spermine form; PDB entry 1D48), base stacking interactions, and crystal and X-ray diffraction and tables containing base pair geometries, conformations of sugar−phosphate backbones, P−P distances in the grooves, polar interactions involving water molecules, and a comparison of crystallization conditions. This material is available free of charge via the Internet at http://pubs.acs.org.

REFERENCES

1. Wang, A. H.-J., Quigley, G. J., Kolpak, F. J., Crawford, J. L., Van Boom, J. H., van der Marel, G. A., and Rich, A. (1979) Molecular structure of a left-handed double helical DNA fragment at atomic resolution, *Nature 282*, 680−686.
2. Pohl, F. M., and Jovin, T. M. (1972) Salt-induced co-operative conformational change of a synthetic DNA: Equilibrium and kinetic studies with poly (dG-dC), *J. Mol. Biol. 67*, 375−396.
3. Nordheim, A., and Rich, A. (1983) The sequence (dC-dA)$_n$·(dG-dT)$_n$ forms left-handed Z-DNA in negatively supercoiled plasmids, *Proc. Natl. Acad. Sci. U.S.A. 80*, 1821−1825.
4. Haniford, D. B., and Pulleyblank, D. E. (1983) Facile transition of poly[d(TG)·d(CA)] into a left-handed helix in physiological conditions, *Nature 302*, 632−634.
5. Kladde, M. P., Kohwi, Y., Kohwi-Shigematsu, T., and Gorski, J. (1994) The non-B-DNA structure of d(CA/TG)n differs from that of Z-DNA, *Proc. Natl. Acad. Sci. U.S.A. 91*, 1898−1902.
6. Ho, P. S. (1994) The non-B-DNA structure of d(CA/TG)$_n$ does not differ from that of Z-DNA, *Proc. Natl. Acad. Sci. U.S.A. 91*, 9549−9553.
7. Peck, L. J., and Wang, J. C. (1983) Energetics of B-to-Z transition in DNA, *Proc. Natl. Acad. Sci. U.S.A. 80*, 6206−6210.
8. Singleton, C. K., Klysik, J., Stirdivant, S. M., and Wells, R. D. (1982) Left-handed Z-DNA is induced by supercoiling in physiological ionic conditions, *Nature 299*, 312−316.
9. Nordheim, A., Pardue, M. L., Lafer, E. M., Moller, A., Stollar, B. D., and Rich, A. (1981) Antibodies to left-handed Z-DNA bind

to interband regions of *Drosophila polytene* chromosomes, *Nature 294*, 417−422.
10. Thamann, T. J., Lord, R. C., Wang, A. H., and Rich, A. (1981) The high salt form of poly(dG-dC)·poly(dG-dC) is left-handed Z-DNA: Raman spectra of crystals and solutions, *Nucleic Acids Res. 9*, 5443−5457.
11. Rahmouni, A. R., and Wells, R. D. (1989) Stabilization of Z DNA in vivo by localized supercoiling, *Science 246*, 358−363.
12. Rich, A., and Zhang, S. (2003) Timeline: Z-DNA: The long road to biological function, *Nat. Rev. Genet. 4*, 566−572.
13. Peck, L. J., Nordheim, A., Rich, A., and Wang, J. C. (1982) Flipping of cloned $d(pCpG)_n$·$d(pCpG)_n$ DNA sequences from right- to left-handed helical structure by salt, Co(III), or negative supercoiling, *Proc. Natl. Acad. Sci. U.S.A. 79*, 4560−4564.
14. Malfoy, B., Rousseau, N., and Leng, M. (1982) Interaction between antibodies to Z-form deoxyribonucleic acid and double-stranded polynucleotides, *Biochemistry 21*, 5463−5467.
15. Jovin, T. M., et al. (1983) Left-handed DNA: From synthetic polymers to chromosomes, *J, Biomol. Struct. Dyn. 1*, 21−57.
16. Behe, M., and Felsenfeld, G. (1981) Effects of methylation on a synthetic polynucleotide: The B−Z transition in poly(dG-m5dC)·poly(dG-m5dC), *Proc. Natl. Acad. Sci. U.S.A. 78*, 1619−1623.
17. Gessner, R. V., Quigley, G. J., Wang, A. H.-J., Van Der Marel, G. A., Van Boom, J. H., and Rich, A. (1985) Structural basis for stabilization of Z-DNA by cobalt hexaammine and magnesium cations, *Biochemistry 24*, 237−240.
18. Egli, M., Williams, L. D., Gao, Q., and Rich, A. (1991) Structure of the pure-spermine form of Z-DNA (magnesium free) at 1-Å resolution, *Biochemistry 30*, 11388−11402.
19. Vorlickova, M., Kypr, J., Stokrova, S., and Sponar, J. (1982) A Z-like form of poly(dA-dC)·poly(dG-dT) in solution? *Nucleic Acids Res. 10*, 1071−1080.
20. Vorlickova, M., Sedlacek, P., Kypr, J., and Sponar, J. (1982) Conformational transitions of poly(dA-dT)poly(dA-dT) in ethanolic solutions, *Nucleic Acids Res. 10*, 6969−6979.
21. Zimmer, C., Tymen, S., Marck, C., and Guschlbauer, W. (1982) Conformational transitions of poly(dA-dC)·poly(dG-dT) induced by high salt or in ethanolic solution, *Nucleic Acids Res. 10*, 1081−1091.
22. Hamada, H., and Kakunaga, T. (1982) Potential Z-DNA forming sequences are highly dispersed in the human genome, *Nature 298*, 396−398.
23. Hamada, H., Petrino, M. G., and Kakunaga, T. (1982) A novel repeated element with Z- DNA-forming potential is widely found in evolutionarily diverse eukaryotic genomes, *Proc. Natl. Acad. Sci. U.S.A. 79*, 6465−6469.
24. Nordheim, A., Lafer, E. M., Peck, L. J., Wang, J. C., Stollar, B. D., and Rich, A. (1982) Negatively supercoiled plasmids contain left-handed Z DNA segments as detected by specific antibody binding, *Cell 31*, 309−318.
25. Murre, C., McCaw, P. S., and Baltimore, D. (1989) A new DNA binding and dimerization motif in immunoglobulin enhancer binding, daughterless, MyoD, and myc proteins, *Cell 56*, 777−783.
26. Drew, H., Takano, T., Tanaka, S., Itakura, K., and Dickerson, R. E. (1980) High-salt d(CpGpCpG), a left-handed Z′ DNA double helix, *Nature 286*, 567−573.
27. Crawford, J. L., Kolpak, F. J., Wang, A. H., Quigley, G. J., van Boom, J. H., van der Marel, G., and Rich, A. (1980) The tetramer d(CpGpCpG) crystallizes as a left-handed double helix, *Proc. Natl. Acad. Sci. U.S.A. 77*, 4016−4020.
28. Coll, M., Fita, I., Lloveras, J., Subirana, J. A., Bardella, F., Huynh-Dinh, T., and Igolen, J. (1988) Structure of d(CACGTG), Z-DNA hexamer containing AT base pairs, *Nucleic Acids Res. 16*, 8695−8705.
29. Harper, A., Brannigan, J. A., Buck, M., Hewitt, L., Lewis, R. J., Moore, M. H., and Schneider, B. (1998) Structure of $d(TGCGCA)_2$ and a comparison to other DNA hexamers, *Acta Crystallogr. D54*, 1273−1284.
30. Thiyagarajan, S., Satheesh Kumar, P., Rajan, S. S., and Gautham, N. (2002) Structure of $d(TGCGCA)_2$ at 293 K: Comparison of the effects of sequence and temperature, *Acta Crystallogr. D58*, 1381−1384.
31. Sadasivan, C., and Gautham, N. (1995) Sequence-dependent microheterogeneity of Z-DNA: The crystal and molecular structures of d(CACGCG)·d(CGCGTG) and d(CGCACG)·d(CGTGCG), *J. Mol. Biol. 248*, 918−930.
32. Karthe, P., and Gautham, N. (1998) Structure of d(CACGCG)·d(CGCGTG) in crystals grown in the presence of ruthenium(III) hexammine chloride, *Acta Crystallogr. D54*, 501−509.
33. Thiyagarajan, S., Rajan, S. S., and Gautham, N. (2004) Cobalt hexammine induced tautomeric shift in Z-DNA: The structure of d(CGCGCA)·d(TGCGCG) in two crystal forms, *Nucleic Acids Res. 32*, 5945−5953.
34. Gessner, R. V., Frederick, C. A., Quigley, G. J., Rich, A., and Wang, A. H.-J. (1989) The molecular structure of the left-handed Z-DNA double helix at 1.0 angstrom atomic resolution. Geometry, conformation, and ionic interactions of d(CGCGCG), *J. Biol. Chem. 264*, 7921−7935.
35. Ganesh, K. N., and Rajendrakumar, G. V. (1990) Conformational studies of $d(CACGTG)_2$ and d(CACCGTG)·d(CACGGTG) by two-dimensional ^1H, ^{31}P NMR and circular dichroism spectra, *Tetrahedron 46*, 1311−1322.
36. Brunger, A. T., Kuriyan, J., and Karplus, M. (1987) Crystallographic R factor refinement by molecular dynamics, *Science 235*, 458−460.
37. Cambillau, C., and Horjales, E. (1987) TOM: A FRODO subpackage for protein−ligand fitting with interactive energy minimization, *J. Mol. Graphics 5*, 174−177.
38. Brunger, A. T. (1992) *X-PLOR version 3.1 Manual: A system for X-ray crystallography & NMR*, Yale University, New Haven, CT.
39. Gessner, R. V., Quigley, G. J., and Egli, M. (1994) Comparative studies of high resolution Z-DNA crystal structures. Part 1: Common hydration patterns of alternating dC-dG, *J. Mol. Biol. 236*, 1154−1168.
40. Kennard, O. (1985) Structural studies of DNA fragments: The G.T wobble base pair in A, B and Z DNA; the G·A base pair in B-DNA, *J. Biomol. Struct. Dyn. 3*, 205−226.
41. Korolev, N., Lyubartsev, A. P., Nordenskiold, L., and Laaksonen, A. (2001) Spermine: An "invisible" component in the crystals of B-DNA. A grand canonical Monte Carlo and molecular dynamics simulation study, *J. Mol. Biol. 308*, 907−917.
42. Woo, N. H., Seeman, N. C., and Rich, A. (1979) Crystal structure of putrescine diphosphate: A model system for amine-nucleic acid interactions, *Biopolymers 18*, 539−552.
43. Arnott, S., Chandrasekaran, R., Birdsall, D. L., Leslie, A. G., and Ratliff, R. L. (1980) Left-handed DNA helices, *Nature 283*, 743−745.
44. Ohishi, H., Kunisawa, S., van der Marel, G., van Boom, J. H., Rich, A., Wang, A. H., Tomita, K., and Hakoshima, T. (1991) Interaction between the left-handed Z-DNA and polyamine. The crystal structure of the $d(CG)_3$ and N-(2-aminoethyl)-1,4-diaminobutane complex, *FEBS Lett. 284*, 238−244.
45. Ohishi, H., Nakanishi, I., Inubushi, K., van der Marel, G., van Boom, J. H., Rich, A., Wang, A. H., Hakoshima, T., and Tomita, K. (1996) Interaction between the left-handed Z-DNA and polyamine-2. The crystal structure of the $d(CG)_3$ and spermidine complex, *FEBS Lett. 391*, 153−156.
46. Ohishi, H., Terasoma, N., Nakanishi, I., van der Marel, G., van Boom, J. H., Rich, A., Wang, A. H., Hakoshima, T., and Tomita, K. (1996) Interaction between left-handed Z-DNA and polyamine. 3. The crystal structure of the $d(CG)_3$ and thermospermine complex, *FEBS Lett. 398*, 291−296.
47. Ohishi, H., Suzuki, K., Ohtsuchi, M., Hakoshima, T., and Rich, A. (2002) The crystal structure of N(1)-[2-(2-amino-ethylamino)-ethyl]-ethane-1,2-diamine(polyamines) binding to the minor groove of $d(CGCGCG)_2$, hexamer at room temperature, *FEBS Lett. 523*, 29−34.
48. Parkinson, G. N., Arvanitis, G. M., Lessinger, L., Ginell, S. L., Jones, R., Gaffney, B., and Berman, H. M. (1995) Crystal and molecular structure of a new Z-DNA crystal form: d[CGT(2-NH_2-A)CG] and its platinated derivative, *Biochemistry 34*, 15487−15495.
49. Dang, L. X., Pearlman, D. A., and Kollman, P. A. (1990) Why do A·T base pairs inhibit Z-DNA formation?, *Proc. Natl. Acad. Sci. U.S.A. 87*, 4630−4634.
50. Wang, A. H.-J., Hakoshima, T., Van Der Marel, G. A., Van Boom, J. H., and Rich, A. (1984) AT base pairs are less stable than GC base pairs in Z-DNA: The crystal structure of d(m^5CGTAm^5-CG), *Cell 37*, 321−331.
51. Bancroft, D., Williams, L. D., Rich, A., and Egli, M. (1994) The low-temperature crystal structure of the pure-spermine form of Z-DNA reveals binding of a spermine molecule in the minor groove, *Biochemistry 33*, 1073−1086.

52. Wang, Y., Thomas, G. A., and Peticolas, W. L. (1987) Sequence dependence of the B to Z transition in crystals and aqueous NaCl solutions for deoxyoligonucleotides containing all four canonical DNA bases, *Biochemistry 26*, 5178−5186.
53. van Dam, L., Korolev, N., and Nordenskiold, L. (2002) Polyamine-nucleic acid interactions and the effects on structure in oriented DNA fibers, *Nucleic Acids Res. 30*, 419−428.
54. Howell, M. L., Schroth, G. P., and Ho, P. S. (1996) Sequence-dependent effects of spermine on the thermodynamics of the B-DNA to Z-DNA transition, *Biochemistry 35*, 15373−15382.
55. Tippin, D. B., and Sundaralingam, M. (1997) Nine polymorphic crystal structures of d(CCGGGCCCGG), d(CCGGGCCm5CGG), d(Cm5CGGGCCm5CGG) and d(CCGGGCC(Br)5CGG) in three different conformations: Effects of spermine binding and methylation on the bending and condensation of A-DNA, *J. Mol. Biol. 267*, 1171−1185.
56. Juranic, Z., Kidric, M., Tomin, R., Juranic, I., Spuzic, I., and Petrovic, J. (1991) The importance of the specific Z-DNA structure and polyamines in carcinogenesis: Fact or fiction, *Med. Hypotheses 35*, 353−357.
57. Urpi, L., et al. (1989) Conformations in crystals and solutions of d(CACGTG), d(CCGCGG) and d(GGCGCC) studied by vibrational spectroscopy, *Nucleic Acids Res. 17*, 6669−6680.
58. Zhou, G., and Ho, P. S. (1990) Stabilization of Z-DNA by demethylation of thymine bases: 1.3 angstroms single-crystal structure of d(m^{5}CGUAm^{5}CG), *Biochemistry 29*, 7229−7236.
59. Fujii, S., Wang, A. H.-J., Van Der Marel, G. A., Van Boom, J. H., and Rich, A. (1982) Molecular structure of (m5DC-DG)$_3$: The role of the methyl group on 5-methyl cytosine in stabilizing Z-DNA, *Nucleic Acids Res. 10*, 7879−7892.
60. Chevrier, B., Dock, A. C., Hartmann, B., Leng, M., Moras, D., Thuong, M. T., and Westhof, E. (1986) Solvation of the left-handed hexamer d(5BrC-G-5BrC-G-5BrC-G) in crystals grown at two temperatures, *J. Mol. Biol. 188*, 707−719.
61. Hua, N., van der Marel, G. A., van Boom, J. H., and Feigon, J. (1989) Non-contiguous regions of Z-DNA in a DNA dodecamer, *Nucleic Acids Res. 17*, 7923−7944.

BI051569L